玉井　克人

発表者氏名	論文タイトル名	発表誌名	巻号	ページ	出版年
Kimura Y., Miyazaki N., Eng M., Hayashi N., Eng M., Otsuru S., Tamai K., and Kaneda Y.	Controlled Release of Bone Morphogenetic Protein-2 Enhances Recruitment of Osteogenic Progenitor Cells for De Novo Generation of Bone Tissue	Tissue Eng Part A	10	1263-1270	2010
Shinbo T., Tanemura A., Yamazaki T., Tamai K., Katayama I., and Kaneda Y.	Serum Anti-BPAG1 Auto-Antibody Is a Novel Marker for Human Melanoma	PLOS ONE	5	E105666	2010
Takemoto H., Tamai K., Akasaka E., Rokunohe D., Takiyoshi N., Umegaki N., Nkajima K., Aizu T., Kaneko T., Nakano H., and Sawamura D.	Relation between the expression levels of the POU transcription factors Skn-1a and Skn-1n and keratinocyte differentiation	Journal of Dermatological Science	60	193-205	2010
Koga H., Hamada T., Ishii N., Fukuda S., Sakaguchi S., Nakano H., Tamai K., Sawamura D., and Hashimoto T.	Exon 87 skipping of the COL7A1 gene in dominant dystrophic epidermolysis bullosa	The Journal of Dermatology	38	489-492	2011
Fujita H., Tamai K., Kawachi M., Saga K., Shimbo T., Yamzaki T., and Kaneda Y.	Methyl-beta cyclodextrin alters the production and infectivity of Sendai virus	Arch Virol	Epub ahead of print	—	2011
Umegaki N., Nakano H., Tamai K., Mitsuhashi Y., Akasaka E., Sawamura D., and Kataya ma I.	Vörner type palmoplantar keratoderma: novel KRT9 mutation associated with knuckle pad-like lesion and recurrent mutation causing digital mutilation	Br J Dermatol	Epub ahead of print	—	2011

江副　幸子

発表者氏名	論文タイトル名	発表誌名	巻号	ページ	出版年
Shibata M, Ezoe S, and Kanakura Y, et al.	Predictability of the response to tyrosine kinase inhibitors via in vitro analysis of Bcr-Abl phosphorylation.	Leukemia Research	Epub		2011
Fujita J, Ezoe S, Kanakura Y, et al	Myeloid neoplasm-related gene abnormalities differentially affect dendritic cell differentiation from murine hematopoietic stem/progenitor cells.	Immunology Letter	136	61-73	2011
Tokunaga M, Ezoe S, Kanakura Y, et al	BCR-ABL but not JAK2 V617F inhibits erythropoiesis through the Ras signal by inducing p21CIP1/WAF1.	J Biol chem	285	31774-31782	2010

橋本　公二

発表者氏名	論文タイトル名	発表誌名	巻号	ページ	出版年
Shirakata Y, Tokumaru S, Sayama K, Hashimoto K	Auto- and cross-induction by betacellulin in epidermal keratinocytes	J Dermatol Sci	58	162-4	2010
Sayama K, Kajiya K, Sugawara K, Sato S, Hirakawa S, Shirakata Y, Hanakawa Y, Dai X, Ishimatsu-Tsuji Y, Metzger D, Chambon P, Akira S, Paus R, Kishimoto J, Hashimoto K	Inflammatory mediator TAK1 regulates hair follicle morphogenesis and anagen induction shown by using keratinocyte-specific TAK1-deficient mice	PLoS One	5	e11275	2010
Sayama K, Yamamoto M, Shirakata Y, Hanakawa Y, Hirakawa S, Dai X, Tohyama M, Tokumaru S, Shin MS, Sakurai H, Akira S, Hashimoto K	E2 Polyubiquitin-conjugating enzyme Ubc13 in keratinocytes is essential for epidermal integrity	J Biol Chem	285	30042-9	2010
Dai X, Sayama K, Tohyama M, Shirakata Y, Hanakawa Y, Tokumaru S, Yang L, Hirakawa S, Hashimoto K	PPARγ mediates innate immunity by regulating the 1α,25-dihydroxyvitamin D3 induced hBD-3 and cathelicidin in human keratinocytes	J Dermatol Sci	60	179-86	2010

片山　一朗

書籍

著者氏名	論文タイトル名	書籍全体の編集者名	書　籍　名	出版社名	出版地	出版年	ページ
金田 眞理	遺伝相談	松田他編	疾病と治療Ⅳ	南江堂	東京	2010	72-73

雑誌

発表者氏名	論文タイトル名	発表誌名	巻号	ページ	出版年
Terao M, Nishida K, Murota H, Katayama I	Clinical effect of tocoretinate on lichen and macular amyloidosis.	J Dermatol.	38(2)	179-84.	2011
Nishioka M, Tanemura A, Yamanaka T, Umegaki N, Tani M, Katayama I, Takemasa I, Sekimoto M, Tomita K, Tamai N	A case of giant squamous cell carcinoma of the buttock possibly arose from syringocystadenoma and invaded to the rectum.	J Skin Cancer	2011; 2011: 213406. Published online 2010 October 18. doi: 10.1155/2011/213406.		
Kira M, Katayama I	Superimposed linear psoriasis.	J Dermatol	37(12)	1063-65	2010
Takahashi Y, Murota H, Tarutani M, Sano S, Okinaga T, Tominaga K, Yano T, Katayama I	A case of juvenile dermatomyositis manifesting inflammatory epidermal nevus-like skin lesions: unrecognized cutaneous manifestation of blaschkitis?	Allergol Int.	59(4)	425-428	2010
Murota H, Kitaba S, Tani M, Wataya-Kaneda M, Azukizawa H, Tanemura A, Umegaki N, Terao M, Kotobuki Y, Katayama I	Impact of Sedetive and Non-Sedetive Antihistamunes on the Impaired Productivity and Quality of Life in Patients with Pruritic Skin Disease.	Allergy International	163	345-354	2010

Hirakawa S, Tanemura A, Mori H, Katayama I, Hashimoto K	Multiple lymphadenopathy as an initial sign of extramammary Paget disease.	Br J Dermatol	164(1)	200-203	2010
Matsui S, Kitaba S, Itoi S, Kijima A, Murota H, Tani M, Katayama I	A case of disseminated DLE complicated by atopic dermatitis and Sjögren's syndrome: link between hypohidrosis and skin manifestations.	Mod Rheumatol	21(1)	101-105	2010
Shima Y, Kuwahara Y, Murota H, Kitaba S, Kawai M, Hirano T, Arimitsu J, Narazaki M, Hagihara K, Ogata A, Katayama I, Kawase I, Kishimoto T, Tanaka T	The skin of patients with systemic sclerosis softened during the treatment with anti-IL-6 receptor antibody tocilizumab.	Rheumatology (Oxford)	49(12)	2408-12	2010
Nishioka M, Tanemura A, Yamanaka T, Tani M, Miura H, Asakura M, Tamai N, Katayama I	Pilomatrix carcinoma arising from pilomatricoma after 10-year senescent period : Immunohistochemical analysis	J Dermatol	37(8)	735-739	2010
Sumikawa Y, Ansai S, Kimura T, Nakamura J, Inui S, Katayama I	Interstitial type granuloma annulare associated with Sjögren's syndrome.	J Dermatol	37(5)	493-495	2010
Terao M, Sakai N, Higashiyama S, Kotobuki Y, Tanemura A, Wataya-Kaneda M, Yutsudo M, Ozono K, Katayama I	Cutaneous symptoms in a patient with cardiofaciocutaneous syndrome and increased ERK phosphorylation in skin fibroblasts.	Br J Dermatol	163(4)	881-884	2010

Takamatsu H, Takegahara N, Nakagawa Y, Tomura M, Taniguchi M, Friedel RH, Rayburn H, Tessier-Lavigne M, Yoshida Y, Okuno T, Mizui M, Kang S, Nojima S, Tsujimura T, Nakatsuji Y, Katayama I, Toyofuku T, Kikutani H, Kumanogoh A	Semaphorins guide the entry of dendritic cells into the lymphatics by activating myosin II.	Nat Immuno	11(7)	594-600	2010
Shimbo T, Tanemura A, Yamazaki T, Tamai K, Katayama I, Kaneda Y	Serum anti-BPAG1 auto-antibody is a novel marker for human melanoma.	PLoS One	May 10; 5(5): e10566	1-8	2010
Murota H, Takahashi A, Nishioka M, Matsui S, Terao M, Kitaba S, Katayama I	Showering reduces atopic dermatitis in elementary school students.	Eur J Dermatol.	20(3)	410-411	2010
Murota H, Abd El-latif MA, Tamura T, Amano T, Katayama I	Olopatadine hydrochloride improves dermatitis score and inhibits scratch behavior in NC/Nga mice.	Int Arch Allergy Immunol	153 (2)	121-132	2010
Hanafusa T, Umegaki N, Yamaguchi Y, Katayama I	Good's syndrome (hypogammaglobulinemia with thymoma) presenting intractable opportunistic infections and hyperkeratotic lichen planus.	J Dermatol	37(2)	171-174	2010

Abd El-Latif MA, Murota H, Terao M, Katayama I	Effects of a 3-hydroxy-3-methyl glutaryl coenzyme A reductase inhibitor and low-density lipoprotein on proliferation and migration of keratinocytes.	Br J Dermatol	163(1)	128-137	2010
Katayama I, Kotobuki Y, Kiyohara E, Murota H	Annular erythema associated with Sjögren's syndrome: review of the literature on the management and clinical analysis of skin lesions.	Mod Rheumatol	20(2)	123-129	2010
Murota H, Kitaba S, Tani M, Wataya-Kaneda M, Katayama I	Effects of nonsedative antihistamines on productivity of patients with pruritic skin diseases.	Allergy	65(7)	929-930	2010
Terao M, Murota H, Kitaba S, Katayama I	Tumor necrosis factor-alpha processing inhibitor-1 inhibits skin fibrosis in a bleomycin-induced murine model of scleroderma.	Exp Dermatol	19(1)	38-43	2010
Nishimura Y, Yamaguchi Y, Tomita Y, Hamada K, Maeda A, Morita A, Katayama I	Epithelioid sarcoma on the foot masquerading as an intractable wound for > 18 years.	Clin Exp Dermatol	35(3)	263-268	2010
田中智子、横関博雄、片山一朗、金田眞理、田村直、菅野範英、吉岡洋、玉田康彦、四宮滋子	原発性局所多汗症診療ガイドライン	日本皮膚科学会雑誌	120	1607-25	2010
山中隆嗣、種村篤、金田眞理、片山一朗、平川聡史、橋本公二	他脳転移を来たした乳 Paget癌の1例：剖検結果と進展様式の考察	皮膚の科学	9 (3)	229-236	2010

金倉　譲

発表者氏名	論文タイトル名	発表誌名	巻号	ページ	出版年
Shibata M, Ezoe S, Kanakura Y, et al.	Predictability of the response to tyrosine kinase inhibitors via in vitro analysis of Bcr-Abl phosphorylation.	Leukemia Research	Epub		2011
Zaki MA, Kanakura Y, Aozasa K., et al.	Presence of B-cell clones in T-cell lymphoma.	Eur J Haematol	85	412-419	2011
Otsuka M, Mizuki M, Kanakura Y, et al.	Constitutively active FGFR3 with Lys650Glu mutation enhances bortezomib sensitivity in plasma cell malignancy.	Anticancer Res	31	113-122	2011
Hashimoto T, Kanakura Y, Komuro I, et al.	Pulmonary arterial hypertension associated with chronic active Epstein-Barr virus infection.	Intern Med	50	119-124	2011
Fujita J, Ezoe S, Kanakura Y, et al.	Myeloid neoplasm-related gene abnormalities differentially affect dendritic cell differentiation from murine hematopoietic stem/progenitor cells.	Immunology Letter	136	61-73	2011
Kanakura Y, Ozawa K, Omine M, et al.	Safety and efficacy of the terminal complement inhibitor eculizumab in Japanese patients with paroxysmal nocturnal hemoglobinuria: the AEGIS clinical trial.	Int J Hematol	93	36-46	2011
Saito Y, Shibayama H, Kanakura Y, et al.	A cell-death-defying factor, anamorsin mediates cell growth through inactivation of PKC and p38MAPK.	Biochem Biophys Res Commun	405	303-307	2011
Wada N, Kanakura Y, Aozasa K, et al.	Epstein-barr virus in diffuse large B-Cell lymphoma in immunocompetent patients in Japan is as low as in Western Countries.	J Med Virol	83	317-321	2011
Kashiwagi H, Kanakura Y, Tomiyama Y, et al	Molecular analysis of a patient with type I Glanzmann thrombasthenia and clinical impact of the presence of anti-αIIbβ3 alloantibodies.	Int J Hematol	93	106-111	2011
Saitoh M, Oritani K, Kanakura Y, et al	Identification of functional domains and novel binding partners of STIM proteins.	J Cell Biochem	112	147-156	2011

Tadokoro S, Tomiyama Y, Kanakura Y, et al	A potential role for α-actinin in inside-out αIIbβ3 signaling.	Blood	117	250-258	2011
Park KA, Kanakura Y, Shibayama H	Nuclear translocation of anamorsin during drug-induced dopaminergic neurodegeneration in culture and in rat brain.	J Neural Transm	118	433-444	2011
Ichii M, Oritani K, Kanakura Y, et al.	The density of CD10 corresponds to commitment and progression in the human B lymphoid lineage.	Int J Hematol	92	111-117	2010
Arita Y, Sakata Y, Kanakura Y, et al	The efficacy of tocilizumab in a patient with pulmonary arterial hypertension associated with Castleman's disease.	Heart Vessels	25	444-447	2010
Tokunaga M, Ezoe S, Kanakura Y, et al	BCR-ABL but not JAK2 V617F inhibits erythropoiesis through the Ras signal by inducing p21CIP1/WAF1.	J Biol Chem	285	31774-31782	2010
Nagai T, Takeuchi J, Kanakura Y, et al	Imatinib for newly diagnosed chronic-phase chronic myeloid leukemia: results of a prospective study in Japan.	Int J Hematol	92	111-117	2010
Ichii M, Oritani K, Kanakura Y, et al	Stromal cell-free conditions favorable for human B lymphopoiesis in culture.	J Immunol Methods.	359	47-55	2010
Wada N, Kohara M, Kanakura Y, et al	Diffuse large B-cell lymphoma in the spinal epidural space: A study of the Osaka Lymphoma Study Group.	Pathol Res Pract	206	439-444	2010

Ⅳ.研究成果の刊行物・別冊

TISSUE ENGINEERING: Part A
Volume 00, Number 00, 2010

DOI: 10.1089/ten.tea.2009.0322

Original Article

Controlled Release of Bone Morphogenetic Protein-2 Enhances Recruitment of Osteogenic Progenitor Cells for *De Novo* Generation of Bone Tissue

Yu Kimura, Ph.D.,[1] Nobuhiko Miyazaki, M.Eng.,[1] Naoki Hayashi, M.Eng.,[1]
Satoru Otsuru, M.D., Ph.D.,[2] Katsuto Tamai, M.D., Ph.D.,[2] Yasufumi Kaneda, M.D., Ph.D.,[2]
and Yasuhiko Tabata, Ph.D., D.Med.Sci., D.Pharm.[1]

The objective of this study was to evaluate the cellular contribution to the phenomenon of *de novo* generation of bone tissue induced by the controlled release of bone morphogenetic protein-2 (BMP-2). Gelatin hydrogels (2 mg) incorporating BMP-2 (3 μg) with different water contents were subcutaneously implanted into the back of enhanced green fluorescent protein-chimeric mice to induce the ectopic *de novo* generation of bone tissue. The hydrogels incorporating BMP-2 could release BMP-2 at different time profiles. When evaluated radiologically and histologically, the ectopic *de novo* generation of bone tissue was induced by the controlled release of BMP-2 from the hydrogels around the hydrogel-implanted site. The relative percentage number of green fluorescent protein- to osteocalcin-positive cells recruited into the *de novo* generated bone tissue depended on the BMP-2 release profile. The higher the percentage, the stronger was the *de novo* generation of bone tissue. These findings indicate that bone marrow-derived osteoblast progenitor cells were recruited from the blood circulation by BMP-2 release and consequently contributed to the ectopic *de novo* generation of bone tissue. It is conceivable that the local concentration of BMP-2 modifies the recruitment profile of progenitor cells with an osteogenic potential around the release site of BMP-2, resulting in regulated volume of *de novo* generated bone tissue.

Introduction

TISSUE ENGINEERING has been vigorously investigated over the last 20 years to experimentally demonstrate the biomedical feasibility of regeneration in medical therapy. The key components are cells, the scaffolds for cells attachment, proliferation, or differentiation, and biosignaling molecules for cell proliferation and differentiation. Various precursor or stem cells have been extensively studied and the mechanisms of their differentiation into specific cell lineages have been clarified recently.[1,2] Among the well-recognized mechanisms, it has been demonstrated that several soluble factors interact with their cellular receptor and subsequently start the intracellular signals required for specific gene expression. In addition, the matrix present around cells, so-called extracellular matrix, also plays an important role in the activation of signals and their biological functions.[3–5]

Recently, some research reports strongly suggest that stem or precursor cells circulating in the blood and body are originally present for hematopoiesis, vascularization, or mesenchymal tissue regeneration.[6–15] Therefore, it is highly conceivable that a promoted recruitment of cells that are inherently present in the body to a body site results in cell-based tissue regeneration at the site. If the *in vivo* recruitment or fate of cells can be regulated by making use of their recruitment mechanism, tissue regeneration based on the cells present in the body can be achieved. We have developed gelatin hydrogels for the controlled release of various biosignaling molecules, such as growth factors, chemokines, and genes, and succeeded in the regeneration and repairing of various tissues.[16] Among them, it is well-known that bone morphogenetic protein-2 (BMP-2) is a strong inducer of bone tissue formation through mesenchymal cell infiltration, differentiation of mesenchymal cells into chondrocytes, diminishment of chondroid tissue, and generation of bone tissue.[17–19] Many researches have been reported for the complete regeneration of bone tissue with BMP-2.[20] In addition, it has been reported that BMP-2 is able to enhance the cells' mobilization.[21] This activity is promising and useful from the viewpoint that tissue regeneration can be achieved through the recruitment of cells originally present in the body.

[1]Department of Biomaterials, Institute for Frontier Medical Sciences, Kyoto University, Kyoto, Japan.
[2]Department of Molecular therapeutics, Graduate School of Medicine, Osaka University, Osaka, Japan.

The objective of this study was to evaluate BMP-2-induced *de novo* generation of bone tissue in terms of cell recruitment. Previous research reports have demonstrated the contribution of bone marrow for bone fracture healing through hematoma formation.[22–25] Although they indicated the possible contribution of growth factors in hematoma or bone marrow cells to fracture healing, the characterization of cells contributing for *de novo* generation of bone tissue was not clarified. In this study, BMP-2 was incorporated into gelatin hydrogels with different degradabilities for the controlled release in different profiles. After the hydrogels incorporating BMP-2 were implanted subcutaneously, ectopic *de novo* generation of bone tissue was evaluated by radiological and histological examinations. We examined the effect of BMP-2 release profile on the recruitment of bone marrow-derived osteoblast progenitor cells at the release site of BMP-2 and the consequent *de novo* generation of bone tissue.

Materials and Methods

Materials

A gelatin sample with an isoelectric point of 9.0 was isolated from the porcine skin by an acidic process of collagen (Nitta Gelatin, Osaka, Japan). $Na^{125}I$ (NEZ-033H, >12.95 GBq/mL) was purchased from Perkin-Elmer Life Sciences (Boston, MA). Other chemicals were obtained from Wako Pure Chemical Industries (Osaka, Japan) and used without further purification.

Preparation of gelatin hydrogels

Chemically crosslinked gelatin hydrogels with glutaraldehyde (GA) were prepared according to a previously reported method.[26] Briefly, aqueous solution of 3 wt% gelatin (pH 5.0) was mixed with GA at a final concentration of 0.16 and 0.09 wt%, respectively, followed by incubation at 4°C for 12 h for gelatin crosslinking. The gelatin hydrogel crosslinked was treated with 0.1 M glycine solution to block the residual aldehyde groups. After washing with double-distilled water for three times, the hydrogels were freeze-dried. The crosslinking extent of prepared hydrogels was evaluated by measuring the water content according to a previously described method.[27] The water contents of hydrogels prepared with higher and lower GA concentrations were 97.5 ± 0.1 and 99.3 ± 0.0 wt%, respectively.

In vivo *release test of BMP-2 from gelatin hydrogels*

All the animal experiments were performed according to the Institutional Guidance of Kyoto University on Animal Experimentation and with permission from the Animal Experiment Committee of the Institute for Frontier Medical Science, Kyoto University. All the surgical procedures were performed under continuous inhalation anesthesia using isoflurane (Forane®; Abbott Japan, Osaka, Japan) with 400 Anesthesia Unit (Univentor, Zejtun, Malta).

Human recombinant BMP-2 (Yamanouchi Pharmaceutical, Tokyo, Japan) was radioiodinated through the conventional chloramine T method as previously described.[28] Briefly, 5 μL of $Na^{125}I$ was added to 200 μL of BMP-2 solution (150 μg/mL) in 0.5 M potassium phosphate buffer (pH 7.5) containing 0.5 M sodium chloride. Then, 0.2 mg/mL of chloramine-T in the same buffer (100 μL) was added to the solution mixture. After agitation at room temperature for 2 min, 100 μL of phosphate-buffered saline (PBS; pH 7.4) containing 0.4 mg of sodium metabisulfate was added to the reaction solution to stop radioiodination. The reaction mixture was passed through a PD-10 desalting column (GE Healthcare Life Sciences, Giles, UK) to remove the uncoupled, free ^{125}I molecules from the ^{125}I-labeled BMP-2 (9.0 μg/mL; removal ratio of free ^{125}I = 97.0%).

PBS containing ^{125}I-labeled BMP-2 (27.4 μL, 9.0 μg/mL) and PBS containing nonlabeled BMP-2 (2.6 μL, 1 mg/mL) were mixed and dropped onto 2 mg of freeze-dried gelatin hydrogels, followed by incubation at 4°C for 12 h, to allow to swell into the hydrogel. Following the implantation of gelatin hydrogels incorporating ^{125}I-labeled BMP-2 into the back subcutis of 6-week-old, female ddY mice (18–20 g body weight; Shimizu Laboratory Supply, Kyoto, Japan), tissue around the implanted site was extracted at different time intervals after hydrogel implantation, and the tissue radioactivity was counted by a gamma counter to estimate the *in vivo* time profiles of BMP-2 release ($n = 3$, at each time point).

Preparation of green fluorescent protein-chimeric mice

C57BL/6 transgenic mice that ubiquitously express enhanced green fluorescent protein (GFP) under the Cyto-Megalovirus (CMV) early enhancer/chicken β actin (CAG) promoter were provided by RIKEN BRC through the National Bio-Resource Project of the MEXT, Japan. Preparation of chimeric mice was performed according to a previously reported procedure.[29] Briefly, bone marrow cells were isolated from 8- to 10-week-old, male transgenic mice under sterile conditions.[30] The cells were incubated with CD90.2 microbeads (no. 130-049-101; Miltenyi Biotec, Auburn, CA) and RPMI 1640 medium at 8°C for 20 min and passed through large depletion (LD) column with Midi MACS system (no. 130-042-901; Miltenyi Biotec) for depletion of CD-90.2-positive T cells and prevention of subsequent autoimmune attack. Eight- to 10-week-old, female C57BL/6 mice were irradiated lethally with 10 Gy of gamma ray. For total bone marrow transplantation, 5×10^6 of bone marrow cells prepared from GFP transgenic mice was intravenously administered to recipient irradiated mice. After the transplantation, the mice were bred for 10 weeks to complete the replacement of bone marrow cells to GFP-positive cells. The replacement ratio of bone marrow cells was 93.2% ± 1.5% when evaluated by the fluorescence-associated cell sorter method (FACS Calibur; BD Bioscience, Franklin Lakes, NJ).

In vivo *assay of* de novo *generation of bone tissue*

BMP-2 was dissolved in PBS at 100 μg/mL and the solution (30 μL) was dropped on the gelatin hydrogel (2 mg) to allow it to swell into the hydrogel. After incubation of the hydrogels incorporating BMP-2 at 4°C for 12 h, the hydrogels were implanted to the back subcutis of GFP-chimeric mice. As a control, gelatin hydrogels incorporating PBS were similarly implanted to the back of the mice. Then, the tissue around the implanted sites was extracted at different time intervals after hydrogel implantation, and the fluorescent images of tissues were obtained by a digital microscope (Multiviewer System VB-S20; Keyence, Osaka, Japan). *De novo* generation of bone tissue was radiologically exam-

ined by a soft X-ray machine (Hitex-100; Hitachi, Tokyo, Japan) at 54 kV and 2.5 mA for 20 s. Then the extracted tissues were fixed with 4% paraformaldehyde at 4°C for 48 h, and the bone tissue was decalcified with PBS containing 9 wt% ethylenediamine tetraacetic acid disodium salt and 10 wt% ethylenediamine tetraacetic acid tetrasodium salt (EDTA solution) at 4°C for 6 days. The EDTA solution was changed every other day. After decalcification, the pellets were equilibrated in PBS containing 15 wt% sucrose for 12 h and then in PBS containing 30 wt% sucrose for 12 h, embedded in Tissue-Tek OCT Compound (Sakura Finetek, Tokyo, Japan), frozen on dry ice, and stored at −80°C. For the histological examinations, 6-μm-thick sections were cut with a cryostat (Leica Microsystems AG, Wetzlar, Germany) at the portion of implanted site as central as possible, followed by staining with hematoxylin and eosin. The area of newly formed bone tissue was assessed in terms of histological image analysis using the computer program Image-Pro Plus 3.01 (Media-Cybernetics, Silver Spring, MD).

Immunofluorescence staining

After washing with PBS, the sections (6 μm thickness) were blocked with a normal goat serum for 1 h at room temperature before incubation with a rabbit polyclonal anti-mouse osteocalcin antibody (1:250; Takara Bio, Shiga, Japan) for 1 h at room temperature. Then the sections were stained with a tetramethylrhodamine-isothiocyanate-conjugated goat anti-rabbit IgG (Molecular Probes, Eugene, OR) for 1 h at room temperature. After washing with PBS, the sections were mounted with Vectashield® (Vector Laboratories, Burlingame, CA). Fluorescent images were obtained using an epifluorescent microscope (AX-80; Olympus, Tokyo, Japan), and the relative percentage number of GFP-positive cells to osteocalcin-positive cells in each image was calculated manually by observing the images. Three areas of interest ($100\times100\,\mu m^2$) were chosen randomly from each fluorescent image (at least four images per each experimental group) and the number of GFP- and osteocalcin-positive cells were counted.

In vitro *migration assay*

Bone marrow cells (3×10^6 cells/cm^2) isolated from the transgenic mice described earlier were plated onto cell culture dish (no. 430167; Corning Incorporated, Corning, NY) with alpha minimum essential medium (αMEM; Sigma-Aldrich, St. Louis, MO) containing 15 vol% fetal bovine serum (FBS) and cultured at 37°C and 5% CO_2–95% air atmospheric pressure. The cells were flushed with PBS at 3 days after seeding to remove unattached blood cells and cultured till subconfluent condition for further experiment. The medium was changed to αMEM without serum at 24 h before the migration assay experiment. The cells were trypsinized and plated onto the HTS® fluoroblok inserts (1.3×10^3 cells/mm^2; Falcon no. 351552 with 8-μm-diameter pore; Becton Dickinson, Franklin Lakes, NJ) with αMEM containing 0.5 vol% FBS. The bottom side of the inserts contacted αMEM containing 15 or 0.5 vol% FBS, 100 ng/mL of recombinant human stromal cell-derived factor-1 (SDF-1; no. 350-NS/CF; R&D systems, Minneapolis, MN), BMP-2, or recombinant human placental growth factor (PlGF; no. 264-PG; R&D systems) with 0.1 vol% bovine serum albumin. After 24 h culture, cells that migrated to the bottom side were counted from fluorescent photographs taken by an epifluorescent microscope (IX-70; Olympus). The number of cells in six images (0.594 mm^2 per each image) were counted.

Statistical analysis

All the results were statistically analyzed by the unpaired Student's *t*-test and $p < 0.05$ was considered to be statistically significant. Data were expressed as the mean ± standard deviation.

Results

De novo *generation of bone tissue by gelatin hydrogels incorporating BMP-2*

Figure 1 shows the time profiles of *in vivo* radioactivity remaining after implantation of gelatin hydrogels incorporating ^{125}I-labeled BMP-2 with different water contents. The gelatin hydrogels with higher water content released BMP-2 faster than those with lower water content.

Figure 2 shows the soft X-ray radiophotographs of implanted sites at 2 weeks after the implantation of gelatin hydrogels incorporating 3 μg of BMP-2 or PBS. A radio-opacity portion was observed at the center of tissues implanted with gelatin hydrogels incorporating BMP-2, although the influence of water content on the extent was not observed. On the contrary, no radio-opacity was observed for the BMP-2-free gelatin hydrogels.

Figure 3a–c shows the histological images of the implanted site at 2 weeks after implantation of the gelatin hydrogels incorporating 3 μg of BMP-2 or PBS. Figure 3d shows the histological image of the implanted site at 7 weeks after implantation of the gelatin hydrogel incorporating BMP-2.

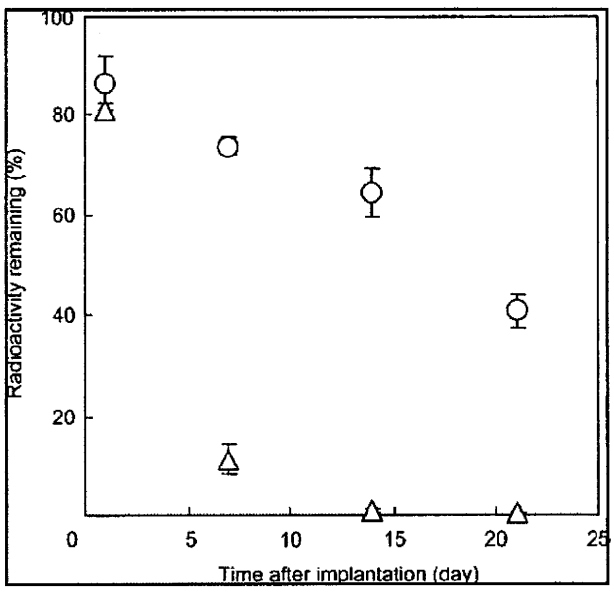

FIG. 1. *In vivo* release profiles of BMP-2 from gelatin hydrogels with water content of 97.5 wt% (○) and 99.3 wt% (Δ). BMP, bone morphogenetic protein.

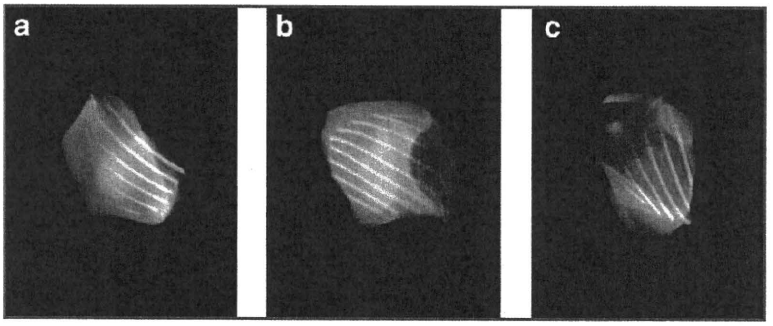

FIG. 2. Soft X-ray radiophotographs of tissues around the implanted site at 2 weeks after implantation of (a) the gelatin hydrogel incorporating BMP-2 (3 μg) with a water content of 97.5 wt%, (b) the gelatin hydrogel incorporating BMP-2 (3 μg) with a water content of 99.3 wt%, and (c) the gelatin hydrogel incorporating PBS with a water content of 97.3 wt%. PBS, phosphate-buffered saline.

After implantation, mature bone tissues with a bone marrow-like structure containing many inflammatory cells, blood cells, and adipocytes (Fig. 3e) were observed. The implanted gelatin hydrogel was completely degraded and was not detected in the section. Figure 4 shows the area of newly formed bone tissue at the implanted site of gelatin hydrogels incorporating BMP-2. After the implantation of gelatin hydrogel incorporating BMP-2 with a water content of 99.3 wt%, the *de novo* generation of bone tissue was observed only at 2 weeks, but thereafter the tissue disappeared. On the contrary, the implantation of hydrogels incorporating BMP-2 with a water content of 97.5 wt% induced significant *de novo* generation of bone tissue and the bone tissue was retained even at 7 weeks after implantation.

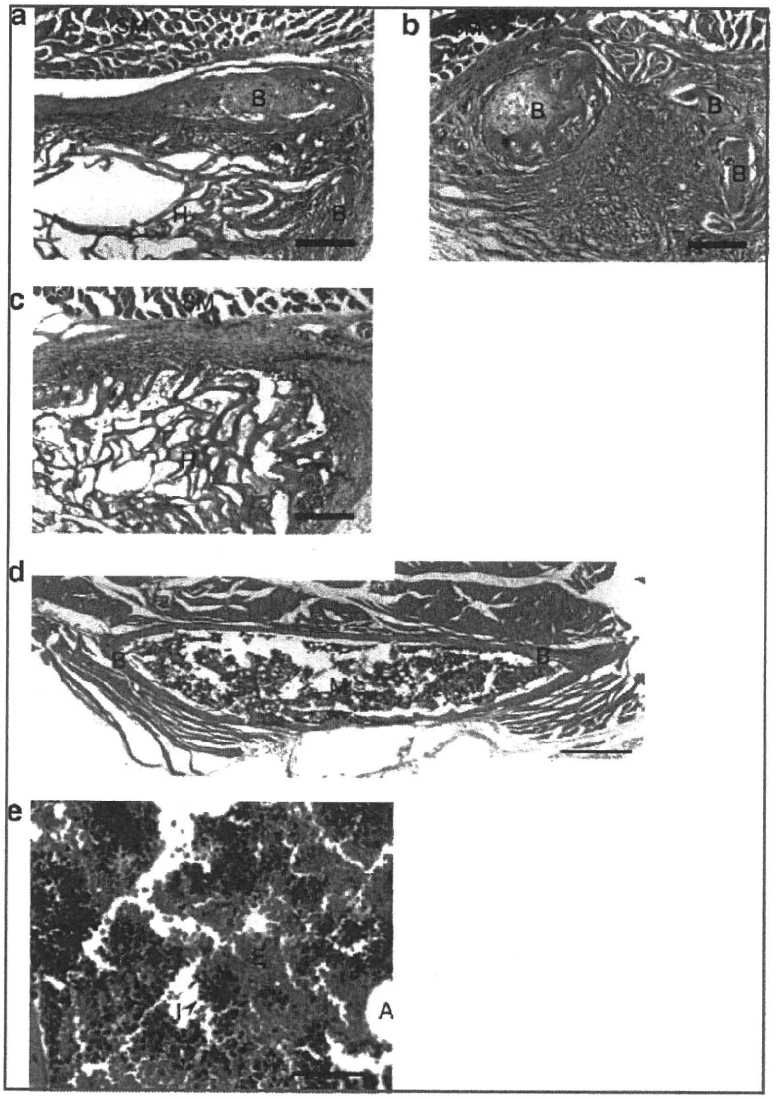

FIG. 3. (a–c) Histological image of tissues around the implanted site at 2 weeks after implantation of (a) the gelatin hydrogel incorporating BMP-2 (3 μg) with a water content of 97.5 wt%, (b) the gelatin hydrogel incorporating BMP-2 (3 μg) with a water content of 99.3 wt%, and (c) the gelatin hydrogel incorporating PBS with a water content of 97.5 wt%. B, bone tissue; M, bone marrow-like structure; SM, subcutaneous muscle tissue; H, remaining gelatin hydrogels. (d) Histological image of tissues around the implanted site at 7 weeks after implantation of gelatin hydrogel incorporating BMP-2 (3 μg) with a water content of 97.5 wt%. Scale bar = 500 μm. (e) Higher magnification image of bone marrow-like structure inside the implanted site. Scale bar = 50 μm. I, inflammatory cells; E, blood cells; A, adipocyte. Color images available online at www.liebertonline.com/ten.

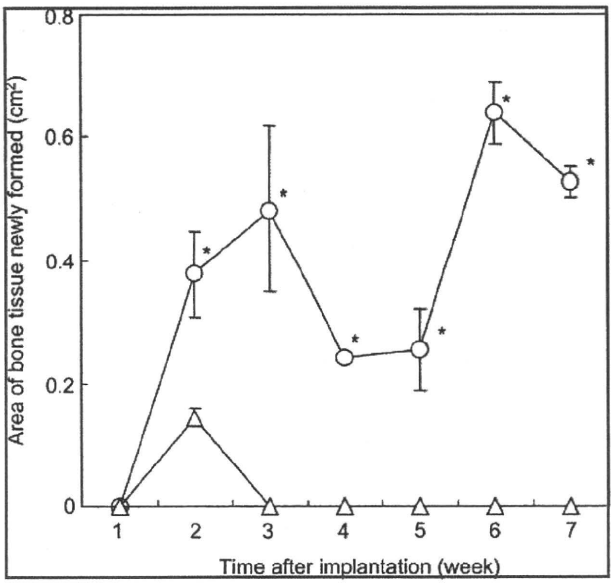

FIG. 4. Area of newly formed bone tissues after implantation of gelatin hydrogels incorporating BMP-2 (3 μg) with a water content of 97.5 wt% (○), gelatin hydrogels incorporating BMP-2 (3 μg) with a water content of 99.3 wt% (Δ). *$p < 0.05$, significant against the area after implantation of gelatin hydrogels incorporating BMP-2 (3 μg) with a water content of 99.3 wt% at the corresponding time.

Recruitment of cells by gelatin hydrogels incorporating BMP-2

Figure 5 shows the fluorescent images of tissues around the implanted site at 2 weeks after the implantation of gelatin hydrogels incorporating BMP-2 or PBS. Irrespective of the experimental groups, a green fluorescence was detected in the implanted sites, which indicates the accumulation of bone marrow-derived cells.

Figure 6 shows the immunofluorescent images of tissues around the implanted site at 2 weeks after implantation of gelatin hydrogels incorporating BMP-2 or PBS. Cells with green fluorescence were observed in all images, and the cells were of round and spindle shape. For the gelatin hydrogels incorporating BMP-2, many red-stained cells were observed around the implanted site (Fig. 6a, b). On the contrary, no cells with red fluorescence were observed around the implanted site of gelatin hydrogels without BMP-2 (Fig. 6c). Figure 7 shows the relative percentage number of GFP-positive cells to osteocalcin-positive cells around the implanted site at 2 weeks after implantation of gelatin hydrogels incorporating BMP-2 or PBS. The implantation of gelatin hydrogels incorporating BMP-2 with different water contents increased the relative percentage number of GFP-positive cells to osteocalcin-positive cells around the implanted site. And the relative percentage for the gelatin hydrogel incorporating BMP-2 with a water content of 97.5 wt% was significantly higher than that of hydrogels with a water content 99.3 wt%. After this time point, it was practically impossible to compare the accumulation of bone marrow-derived cells between the implanted sites of the gelatin hydrogel incorporating BMP-2 with water contents of 97.5 and 99.3 wt%. This is due to the disappearance of the newly formed bone tissue around the implanted site of the latter gelatin hydrogel incorporating BMP-2.

In vitro *cell migration*

Figure 8 shows the number of cells that migrated to the bottom side of the inserts at 24 h after incubation with αMEM containing BMP-2 or other factors. No activity as a chemoattractant to bone marrow cells was observed for BMP-2. The migration level was the same as that of the negative control (0.5 vol% FBS). However, a strong chemoattractant activity was observed for SDF-1 and PlGF, which was the same as that of the positive control (15 vol% FBS). The activity by PlGF was significantly higher than that by SDF-1 and 15 vol% FBS.

Discussion

This study demonstrates that the BMP-2 release profile affected the extent of accumulation of bone marrow-derived cells and the consequent *de novo* generation of bone tissues. The hydrogel water contents of 97.5 and 99.3 wt% indicated that the weight ratio of gelatin molecules to total hydrogel were 2.5 and 0.7 wt%. The difference in gelatin molecule fraction and crosslinking density of hydrogels caused the difference in hydrogel degradation and the consequent BMP-2 *in vivo* release profiles (Fig. 1). The BMP-2 release for a longer time period enabled strong accumulation of GFP-positive bone marrow-derived osteoblast progenitor cells which are also stained with the anti-osteocalcin antibody, even at 2 weeks after implantation. It is apparent from Figure 5 that the accumulation of bone marrow-derived cells was observed by the implantation of gelatin hydrogels with or without BMP-2. However, from the double-staining assay, for the hydrogel without BMP-2, no osteocalcin-positive cells were detected around the implanted site (Figs. 6 and 7). As

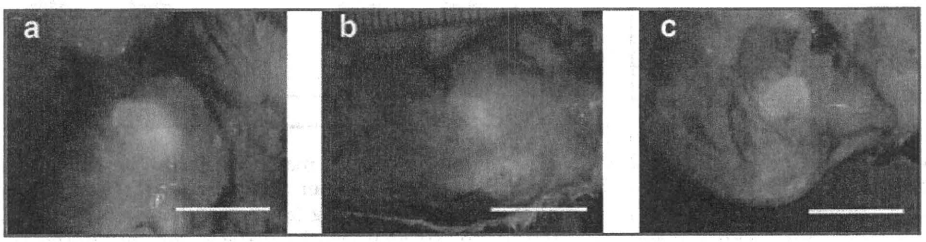

FIG. 5. Fluorescent images of the area surrounding the implant at 2 weeks after implantation of (**a**) the gelatin hydrogel incorporating BMP-2 (3 μg) with a water content of 97.5 wt%, (**b**) the gelatin hydrogel incorporating BMP-2 (3 μg) with a water content of 99.3 wt%, and (**c**) the gelatin hydrogel incorporating PBS with a water content of 97.3 wt%. Scale bar = 1 cm. Color images available online at www.liebertonline.com/ten.

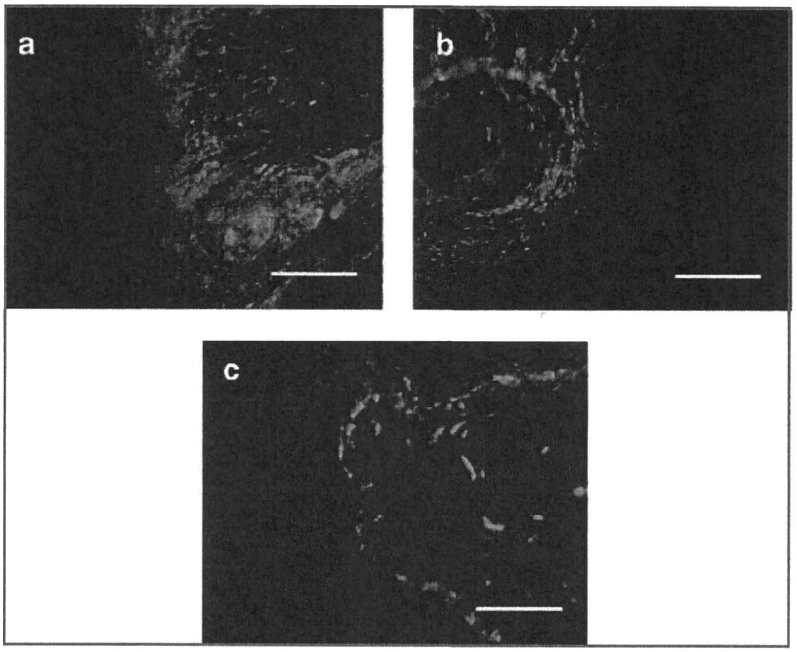

FIG. 6. Immunofluorescence staining images of tissue around the implanted site at 2 weeks after implantation of (a) the gelatin hydrogel incorporating BMP-2 (3 μg) with a water content of 97.5 wt%, (b) the gelatin hydrogel incorporating BMP-2 (3 μg) with a water content of 99.3 wt%, and (c) the gelatin hydrogel incorporating PBS with a water content of 97.3 wt%. Red fluorescence: osteocalcin; green fluorescence: green fluorescent protein. Scale bar = 200 μm. Color images available online at www.liebertonline.com/ten.

the osteocalcin-expressing cells are generally osteoblastic cells with bone formation activity, we can say with certainty that the BMP-2 release increased the recruitment of osteogenic cells around the release site.

The extent of *de novo* generation of bone tissue depended on the water content of gelatin hydrogels. This finding was experimentally confirmed in a previous study[26] and the present results are also in accordance to it even after extended time course (7 weeks after implantation). The decrease in the *de novo* generated area was observed in 4 or 5 and 3 weeks after implantation for gelatin hydrogels with water contents of 97.5 and 99.3 wt%, respectively (Fig. 4). This time profile can be explained in terms of that of BMP-2 release. For the gelatin hydrogel, the time profile of BMP-2 release was well correlated to that of hydrogel degradation. The hydrogel that is degraded for 4–5 weeks would release

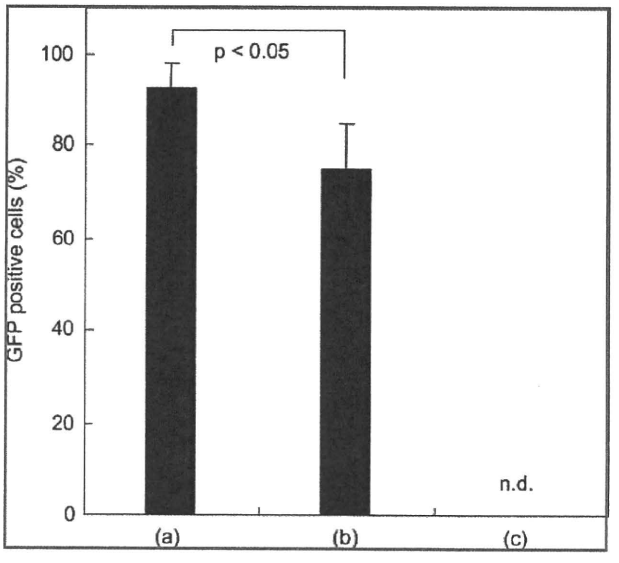

FIG. 7. Relative percentage number of GFP-positive cells to osteocalcin-positive cells around the implanted site at 2 weeks after implantation of (a) gelatin hydrogels incorporating BMP-2 (3 μg) with a water content of 97.5 wt%, (b) gelatin hydrogels incorporating BMP-2 (3 μg) with a water content of 99.3 wt%, and (c) gelatin hydrogels incorporating PBS with a water content of 97.5 wt%. n.d., not detected; GFP, green fluorescent protein.

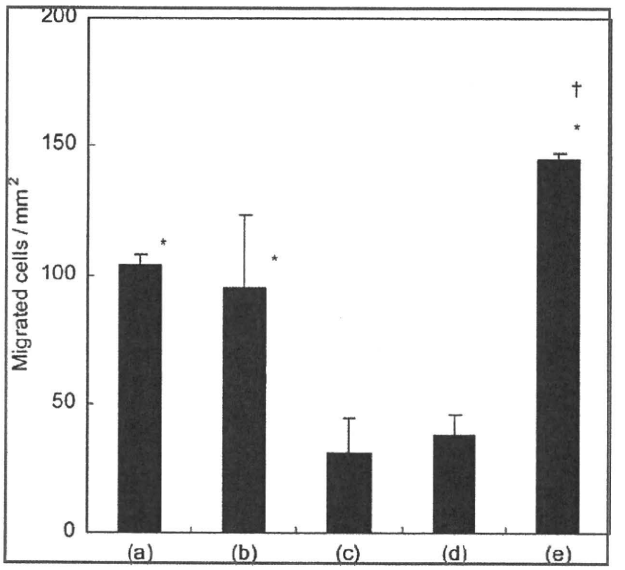

FIG. 8. Migration of bone marrow cells through the transwell membrane at 24 h after incubation with α-minimum essential medium containing (a) 15 vol% fetal bovine serum, (b) 100 ng/mL stromal cell-derived factor-1, (c) 100 ng/mL BMP-2, (d) 0.5 vol% fetal bovine serum, and (e) 100 ng/mL placental growth factor. $^*p < 0.05$ against the groups (c) and (d); $^\dagger p < 0.05$ significant against the groups (a) and (b).

BMP-2 for 4–5 weeks. It is possible that for this range, the BMP-2 release results in the BMP-induced *de novo* generation of bone tissue. However, the cessation of release would suppress bone tissue induction, resulting in the disappearance of bone tissue. The area of *de novo* generated bone increased again from 6 weeks after implantation. The cells recruited by the released and remaining BMP-2 may be able to further promote *de novo* generation of bone tissue. This reason is not clear at present.

Significant difference in the accumulation of osteocalcin-positive cells between the gelatin hydrogels with water contents of 97.5 and 99.3 wt% was observed (Fig. 6). This experimental result indicates that the profile of BMP-2 release affects the recruitment of bone marrow-derived cells. It is conceivable that BMP-2 release for a longer time period induces the recruitment of cells for a long time period, resulting in enhanced accumulation of cells. BMP-2 can accelerate bone tissue formation[18] through osteoblast migration,[31] by promoting osteogenic differentiation of mesenchymal stem cells,[32,33] angiogenesis,[34] apoptosis of osteoblast,[35] and recruitment of osteoblast progenitor cells.[21,29] It has been demonstrated that BMP-2 could induce the expression of PlGF. The enhanced expression of PlGF promoted the recruitment of progenitor cells from the bone marrow.[36–38] In addition, fibrous tissue and hypertrophic cartilage formation was observed in a fracture healing model of PlGF-deficient mice.[37] The chemoattractant study revealed that PlGF accelerated the migration of isolated bone marrow cells, in contrast to BMP-2 (Fig. 8). It is highly conceivable that BMP-2 functions as a trigger molecule to induce PlGF for the migration of bone marrow-derived cells. Further analysis is needed to understand the effect of BMP-2 release on cell recruitment.

This study clearly indicates that the BMP-2-releasing materials enhance cell accumulation for *de novo* generation of bone tissue. This activity could be modified by the release profile. This finding opens a new strategy of tissue engineering to achieve tissue regeneration by induction of cells present in the body.

Disclosure Statement

No competing financial interests exist.

References

1. Langer, R. Tissue engineering: perspectives, challenges, and future directions. Tissue Eng **13,** 1, 2007.
2. Morrison, S.J., and Spradling, A.C. Stem cells and niches: mechanisms that promote stem cell maintenance throughout life. Cell **132,** 598, 2008.
3. Ingber, D.E., Mow, V.C., Butler, D., Niklason, L., Huard, J., Mao, J., Yannas, I., Kaplan, D., and Vunjak-Novakovic, G. Tissue engineering and developmental biology: going biomimetic. Tissue Eng **12,** 3265, 2006.
4. Matsumoto, T., and Mooney, D.J. Cell instructive polymers. Adv Biochem Eng Biotechnol **102,** 113, 2006.
5. Badylak, S.F. The extracellular matrix as a biologic scaffold material. Biomaterials **28,** 3587, 2007.
6. Ceradini, D.J., Kulkarni, A.R., Callaghan, M.J., Tepper, O.M., Bastidas, N., Kleinman, M.E., Capla, J.M., Galiano, R.D., Levine, J.P., and Gurtner, G.C. Progenitor cell trafficking is regulated by hypoxic gradients through HIF-1 induction of SDF-1. Nat Med **10,** 858, 2004.
7. Eghbali-Fatourechi, G.Z., Lamsam, J., Fraser, D., Nagel, D., Riggs, B.L., and Khosla, S. Circulating osteoblast-lineage cells in humans. N Engl J Med **352,** 1959, 2005.
8. Grunewald, M., Avraham, I., Dor, Y., Bachar-Lustig, E., Itin, A., Yung, S., Chimenti, S., Landsman, L., Abramovitch, R., and Keshet, E. VEGF-induced adult neovascularization: recruitment, retention, and role of accessory cells. Cell **124,** 175, 2006.
9. Jin, D.K., Shido, K., Kopp, H.G., Petit, I., Shmelkov, S.V., Young, L.M., Hooper, A.T., Amano, H., Avecilla, S.T., Heissig, B., Hattori, K., Zhang, F., Hicklin, D.J., Wu, Y., Zhu, Z., Dunn, A., Salari, H., Werb, Z., Hackett, N.R., Crystal, R.G., Lyden, D., and Rafii, S. Cytokine-mediated deployment of SDF-1 induces revascularization through recruitment of $CXCR4^+$ hemangiocytes. Nat Med **12,** 557, 2006.
10. Karp, J.M., and Leng Teo, G.S. Mesenchymal stem cell homing: the devil is in the details. Cell Stem Cell **4,** 206, 2009.
11. Kuznetsov, S.A., Mankani, M.H., Gronthos, S., Satomura, K., Bianco, P., and Robey, P.G. Circulating skeletal stem cells. J Cell Biol **153,** 1133, 2001.
12. Wan, C., He, Q., and Li, G. Allogenic peripheral blood derived mesenchymal stem cells (MSCs) enhance bone regeneration in rabbit ulna critical-sized bone defect model. J Orthop Res **24,** 610, 2006.
13. Wragg, A., Mellad, J.A., Beltran, L.E., Konoplyannikov, M., San, H., Boozer, S., Deans, R.J., Mathur, A., Lederman, R.J., Kovacic, J.C., and Boehm, M. VEGFR1/CXCR4-positive progenitor cells modulate local inflammation and augment tissue perfusion by a SDF-1-dependent mechanism. J Mol Med **86,** 1221, 2008.
14. Zhou, B., Han, Z.C., Poon, M.C., and Pu, W. Mesenchymal stem/stromal cells (MSC) transfected with stromal derived factor 1 (SDF-1) for therapeutic neovascularization: enhancement of cell recruitment and entrapment. Med Hypotheses **68,** 1268, 2007.
15. Zhu, W., Boachie-Adjei, O., Rawlins, B.A., Frenkel, B., Boskey, A.L., Ivashkiv, L.B., and Blobel, C.P. A novel regulatory role for stromal-derived factor-1 signaling in bone morphogenic protein-2 osteogenic differentiation of mesenchymal C2C12 cells. J Biol Chem **282,** 18676, 2007.
16. Tabata, Y. Significance of release technology in tissue engineering. Drug Discov Today **10,** 1639, 2005.
17. Reddi, A.H. Bone morphogenetic proteins: from basic science to clinical applications. J Bone Joint Surg Am **83-A Suppl 1,** S1, 2001.
18. Wozney, J.M. Overview of bone morphogenetic proteins. Spine **27,** S2, 2002.
19. Wozney, J.M., Rosen, V., Celeste, A.J., Mitsock, L.M., Whitters, M.J., Kriz, R.W., Hewick, R.M., and Wang, E.A. Novel regulators of bone formation: molecular clones and activities. Science **242,** 1528, 1988.
20. Bessa, P.C., Casal, M., and Reis, R.L. Bone morphogenetic proteins in tissue engineering: the road from laboratory to clinic, part II (BMP delivery). J Tissue Eng Regen Med **2,** 81, 2008.
21. Otsuru, S., Tamai, K., Yamazaki, T., Yoshikawa, H., and Kaneda, Y. Bone marrow-derived osteoblast progenitor cells in circulating blood contribute to ectopic bone formation in mice. Biochem Biophys Res Commun **354,** 453, 2007.
22. Bruder, S.P., Fink, D.J., and Caplan, A.I. Mesenchymal stem cells in bone development, bone repair, and skeletal regeneration therapy. J Cell Biochem **56,** 283, 1994.
23. Colnot, C., Huang, S., and Helms, J. Analyzing the cellular contribution of bone marrow to fracture healing using bone marrow transplantation in mice. Biochem Biophys Res Commun **350,** 557, 2006.

24. Ozaki, A., Tsunoda, M., Kinoshita, S., and Saura, R. Role of fracture hematoma and periosteum during fracture healing in rats: interaction of fracture hematoma and the periosteum in the initial step of the healing process. J Orthop Sci **5**, 64, 2000.
25. Utvag, S.E., Grundnes, O., and Reikeras, O. Effects of degrees of reaming on healing of segmental fractures in rats. J Orthop Trauma **12**, 192, 1998.
26. Yamamoto, M., Takahashi, Y., and Tabata, Y. Controlled release by biodegradable hydrogyels enhances the ectopic bone formation of bone morphogenetic protein. Biomaterials **24**, 4375, 2003.
27. Tabata, Y., Nagano, A., Muniruzzaman, M., and Ikada, Y. *In vitro* sorption and desorption of basic fibroblast growth factor from biodegradable hydrogels. Biomaterials **19**, 1781, 1998.
28. Ozeki, M., and Tabata, Y. *In vivo* degradability of hydrogels prepared from different gelatins by various cross-linking methods. J Biomater Sci Polym Ed **16**, 549, 2005.
29. Otsuru, S., Tamai, K., Yamazaki, T., Yoshikawa, H., and Kaneda, Y. Circulating bone marrow-derived osteoblast progenitor cells are recruited to the bone-forming site by the CXCR4/stromal cell-derived factor-1 pathway. Stem Cells **26**, 223, 2008.
30. Okabe, M., Ikawa, M., Kominami, K., Nakanishi, T., and Nishimune, Y. Green mice as a source of ubiquitous green cells. FEBS Lett **407**, 313, 1997.
31. Sotobori, T., Ueda, T., Myoui, A., Yoshioka, K., Nakasaki, M., Yoshikawa, H., and Itoh, K. Bone morphogenetic protein-2 promotes the haptotactic migration of murine osteoblastic and osteosarcoma cells by enhancing incorporation of integrin beta1 into lipid rafts. Exp Cell Res **312**, 3927, 2006.
32. Wagner, T.U. Bone morphogenetic protein signaling in stem cells—one signal, many consequences. FEBS J **274**, 2968, 2007.
33. Bessa, P.C., Pedro, A.J., Klosch, B., Nobre, A., van Griensven, M., Reis, R.L., and Casal, M. Osteoinduction in human fat-derived stem cells by recombinant human bone morphogenetic protein-2 produced in *Esclerichia coli*. Biotechnol Lett **30**, 15, 2008.
34. Deckers, M.M., van Bezooijen, R.L., van der Horst, G., Hoogendam, J., van Der Bent, C., Papapoulos, S.E., and Lowik, C.W. Bone morphogenetic proteins stimulate angiogenesis through osteoblast-derived vascular endothelial growth factor A. Endocrinology **143**, 1545, 2002.
35. Hay, E., Lemonnier, J., Fromigue, O., and Marie, P.J. Bone morphogenetic protein-2 promotes osteoblast apoptosis through a Smad-independent, protein kinase C-dependent signaling pathway. J Biol Chem **276**, 29028, 2001.
36. Marrony, S., Bassilana, F., Seuwen, K., and Keller, H. Bone morphogenetic protein 2 induces placental growth factor in mesenchymal stem cells. Bone **33**, 426, 2003.
37. Maes, C., Coenegrachts, L., Stockmans, I., Daci, E., Luttun, A., Petryk, A., Gopalakrishnan, R., Moermans, K., Smets, N., Verfaillie, C.M., Carmeliet, P., Bouillon, R., and Carmeliet, G. Placental growth factor mediates mesenchymal cell development, cartilage turnover, and bone remodeling during fracture repair. J Clin Invest **116**, 1230, 2006.
38. Fiedler, J., Leucht, F., Waltenberger, J., Dehio, C., and Brenner, R.E. VEGF-A and PlGF-1 stimulate chemotactic migration of human mesenchymal progenitor cells. Biochem Biophys Res Commun **334**, 561, 2005.

Address correspondence to:
Yasuhiko Tabata, Ph.D., D.Med.Sci., D.Pharm.
Department of Biomaterials
Institute for Frontier Medical Sciences
Kyoto University
53 Kawara-cho Shogoin
Sakyo-ku
Kyoto 6068507
Japan

E-mail: yasuhiko@frontier.kyoto-u.ac.jp

Received: May 13, 2009
Accepted: November 3, 2009
Online Publication Date: December 15, 2009

OPEN ACCESS Freely available online

PLoS one

Serum Anti-BPAG1 Auto-Antibody Is a Novel Marker for Human Melanoma

Takashi Shimbo[1], Atsushi Tanemura[2], Takehiko Yamazaki[1], Katsuto Tamai[1], Ichiro Katayama[2], Yasufumi Kaneda[1]*

1 Division of Gene Therapy Science, Osaka University Graduate School of Medicine, Osaka, Japan, **2** Department of Dermatology, Osaka University Graduate School of Medicine, Osaka, Japan

Abstract

Malignant melanoma is one of the most aggressive types of tumor. Because malignant melanoma is difficult to treat once it has metastasized, early detection and treatment are essential. The search for reliable biomarkers of early-stage melanoma, therefore, has received much attention. By using a novel method of screening tumor antigens and their auto-antibodies, we identified bullous pemphigoid antigen 1 (BPAG1) as a melanoma antigen recognized by its auto-antibody. BPAG1 is an auto-antigen in the skin disease bullous pemphigoid (BP) and anti-BPAG1 auto-antibodies are detectable in sera from BP patients and are used for BP diagnosis. However, BPAG1 has been viewed as predominantly a keratinocyte-associated protein and a relationship between BPAG1 expression and melanoma has not been previously reported. In the present study, we show that bpag1 is expressed in the mouse F10 melanoma cell line *in vitro* and F10 melanoma tumors *in vivo* and that BPAG1 is expressed in human melanoma cell lines (A375 and G361) and normal human melanocytes. Moreover, the levels of anti-BPAG1 auto-antibodies in the sera of melanoma patients were significantly higher than in the sera of healthy volunteers ($p<0.01$). Furthermore, anti-BPAG1 auto-antibodies were detected in melanoma patients at both early and advanced stages of disease. Here, we report anti-BPAG1 auto-antibodies as a promising marker for the diagnosis of melanoma, and we discuss the significance of the detection of such auto-antibodies in cancer biology and patients.

Citation: Shimbo T, Tanemura A, Yamazaki T, Tamai K, Katayama I, et al. (2010) Serum Anti-BPAG1 Auto-Antibody Is a Novel Marker for Human Melanoma. PLoS ONE 5(5): e10566. doi:10.1371/journal.pone.0010566

Editor: Vladimir Brusic, Dana-Farber Cancer Institute, United States of America

Received January 6, 2010; **Accepted** April 19, 2010; **Published** May 10, 2010

Funding: This work is supported by the Biomedical Cluster Kansai project, which is promoted by the Knowledge Cluster Initiative of the Ministry of Education, Culture, Sports, Science and Technology (http://www.mext.go.jp/). The funders had no role in study design, data collection and analysis, decision to publish, or preparation of the manuscript.

Competing Interests: The authors have declared that no competing interests exist.

* E-mail: kaneday@gts.med.osaka-u.ac.jp

Introduction

Melanoma is one of the most aggressive tumors due to its strong capacity to metastasize. In the United States, there were an estimated 62,480 new melanoma cases and 8,420 deaths caused by melanomas in 2008 [1]. Although the 5-year survival rate of patients with early stage localized melanoma is greater than 90%, survival rates drop to less than 20% once the melanoma has metastasized to distant sites [1]. In general, early diagnosis of cancers greatly improves the survival of patients. Therefore, great efforts have been made to screen tumor markers for early diagnosis. Several melanoma markers (e.g. gp100, MART-1 and tyrosinase) have been detected and proposed for immunotherapy approaches [2,3,4]. With regards to melanoma markers in serum, S100 protein, 5-S-cysteinyldopa and 6-hydroxy-5-methoxyindole-2-carboxylic acid can be useful although levels tend to be more up-regulated in advanced melanomas. As such, these particular markers are not suitable for the early detection of malignant melanoma [5]. Glypican-3 (GPC3), however, is overexpressed in melanoma and its serum concentration can serve as an early stage melanoma diagnostic marker [6,7]. Nevertheless, from a practical prospective, use of only one biomarker may lack sensitivity and specificity and diminish clinicopathologic value. The availability of multiple markers would make the diagnosis of melanoma more reliable, and thus there is a need to identify and assess additional melanoma markers.

In the present study, we developed a screening method to detect tumor markers recognized by auto-antibodies to these proteins in serum. Using this method, we found that bullous pemphigoid antigen 1 (BPAG1) was expressed in both melanoma cell lines and normal melanocytes. BPAG1 is a plakin family protein that anchors keratin filaments to hemidesmosomes [8]. Another protein BPAG2, a transmembranous collagen, is also expressed in the skin and is a component of hemidesmosomes [8]. Deletion of the *dst* gene, that encodes bpag1, disrupts hemidesmosomes structure, resulting in the failure of hemidesmosomes to associate with keratin filaments [9]. Both BPAG1 and BPAG2 can serve as auto-antigens in bullous pemphigoid (BP) [10,11,12]. Auto-antibodies to BPAG1 and BPAG2 maybe detected in the sera of BP patients, and assessment of antibody levels can be used for BP diagnosis and clinical management. While passive transfer experiments have shown that BPAG2 antibodies have pathogenic relevance to BP, the clinicopathological significance of BPAG1 antibodies, has not yet been fully elucidated [13]. It has been hypothesized that anti-BPAG1 auto-antibodies might interfere with hemidesmosome integrity, but this has not been proven [9].

Here, we show that the level of auto-antibodies against BPAG1 in the sera of melanoma patients, at both early and advanced

stages, was significantly higher than levels in the sera of healthy volunteers. These findings identify anti-BPAG1 auto-antibodies as a novel and promising tumor biomarker in the detection of melanoma.

Materials and Methods

Libraries, bacteria and helper phage

The human single-fold scFv libraries I + J (Tomlinson I + J), *E. coli* TG1 and HB2151, and KM13 helper phage were all kindly provided by the Medical Research Council (MRC). The scFv library was prepared as previously described [14]. The scFv library was cloned into the pIT2 expression vector, which contains a lac promoter and a pelB leader sequence upstream of the VH-$(G_4S)_3$-VL insert; the insert is followed by 6×His and myc tags, an amber stop codon and the gene encoding the pIII phage coat protein. Thus, in a suitable non-suppressor strain (HB2151), addition of isopropyl-thio-β-D-galactoside (IPTG) induces only scFv and not scFv–pIII fusion expression.

Mice

Female C57BL/6N mice (6 weeks old) were studied (Charles River Laboratories Japan, Inc., Japan) Animal experiments were performed in accordance with the guidelines of the Osaka University Graduate School of Medicine.

Cell lines and culture

Mouse melanoma cell line F10, mouse fibroblast cell line NIH-3T3, human melanoma cell lines A375, G361 and human epidermoid carcinoma A431 were obtained from the American Type Culture Collection (ATCC, USA). Normal human keratinocyte (NHK) cells and melanocyte (NHM) cells were obtained from Lonza (USA). F10, NIH-3T3, A375, G361 and A431 cells were maintained in Dulbecco's modified Eagle's medium (DMEM) (Nacalai Tesque Inc., Japan). DMEM was supplemented with 10% fetal bovine serum (FBS) (Biowest, France), 100 units/ml penicillin and 0.1 mg/ml streptomycin (penicillin-streptomycin mixed solution) (Nacalai). NHK and NHM cells were maintained in keratinocyte growth medium (KGM) (Lonza) and melanocyte growth medium (MGM-4) (Lonza), respectively.

Preparation of tumor lysates and the isolation of sera from tumor-bearing mice

F10 cells (5×10^6) were intradermally injected into the backs of C57BL/6N mice. After 4 weeks, tumors were excised, and protein was extracted using T-PER Tissue Protein Extraction Reagent (Pierce, USA), according to the manufacturer's instructions. At the same time as the tumor excision, whole blood was collected, and the sera were isolated using Capiject Capillary Blood Collection Tubes (Terumo Corp., Japan).

In vivo screening of tumor-homing phages and isolation of the tumor-binding scFv

F10 cells (5×10^6) were intradermally injected into the backs of C57BL/6N mice. After tumors reached 7 to 8 mm in diameter, we injected the phage library (1×10^{13} CFU) dissolved in 100 μl saline into the tail veins of tumor-bearing mice. After 15 min, the animals were sacrificed by an overdose of anesthetic and perfused via the heart with 100 ml of PBS [15]. Next, the tumor tissue was snap-frozen in liquid nitrogen and homogenized in a mortar. Tumor-homing phages were eluted by using 500 μl of 0.1 M glycine (pH 2.2) for 15 min, and then the solution was neutralized with 50 μl of 2 M Tris-HCl (pH 8). Next, 50 μL of Protein A (GE Healthcare, USA) was added to the neutralized phage solution, and the mixture was rotated for 1.5 h at 4°C. After washing with PBS to remove unbound phages, phages bound to protein A were used to infect log-phase HB2151 for 1 h at 37°C; then, the cells were plated on 2×YT agar plates containing 100 μg/ml carbenicillin. After 16 h of incubation at 37°C, a nitrocellulose membrane soaked in 100 mM IPTG (Takara Bio Inc., Japan) for 10 min was placed on the 2×YT plate for 4 h at 37°C. The plate was stored at 4°C as a master plate for *E.coli* recovery. The membrane was washed 3 times with PBS containing 0.1% tween 20 and blocked 30 min with PBS containing 5% skim milk (Nacalai). Then, the membrane was incubated with tumor lysate followed by tumor-bearing mouse serum. The complexes of auto-antibodies bound to tumor proteins were detected with the anti-mouse IgG horseradish peroxidase-conjugated antibody (GE Healthcare) followed by ECL Western Blotting Kit (GE Healthcare).

Identification of tumor antigen with MALDI-TOF mass spectrometry

Positive clones that were recovered from the stored 2×YT agar plate were re-plated onto a fresh 2×YT agar plate and incubated for 16 h at 37°C. Next, a nitrocellulose membrane soaked with 100 mM IPTG was placed onto the 2×YT agar plate for 4 h at 37°C. After washing with PBS containing 0.1% tween 20, the membrane was blocked 30 min with 0.5% polyvinylpyrrolidone K30 (Nacalai), and then the membrane was incubated with tumor lysate. The scFv-tumor protein complexes were stained with 0.5% ponceau (Wako Pure Chemical Industries, Ltd., Japan)/5% acetic acid in distilled water, and the membrane around the area was excised. The protein on the excised membrane was digested with 100 ng/ml trypsin (Sigma-Aldrich, USA)/40 mM ammonium bicarbonate (Nacalai) for 6 h at 37°C. Then, the solution was dried up, and saturated α-cyano-4-hydroxy cinnamic acid (Wako), 1% trifluoroacetic acid, and 50% acetonitrile was added. After desalting with a ZipTip C18, the solution was analyzed using an Ultraflex MALDI-TOF/TOF instrument (Bruker Daltonik, Germany). The mass spectrometry data were analyzed with the Mascot search engine (http://www.matrixscience.com).

RT-PCR and real-time PCR

RNA was extracted using Isogen (Nippon Gene, Japan), and 1 μg of total RNA was converted to cDNA with SuperScript III (Invitrogen, USA), according to the manufacturer's instructions. Mouse bullous pemphigoid antigen 1 (bpag1), TBC1 domain family member 13 (tbc1d13), uncharacterized protein C7orf30 homolog (c7orf30), and β-actin were amplified using SYBR Premix Ex Taq (Takara Bio) and an ABI Prism 7900 sequence detector (Applied Biosystems, USA). Human BPAG1, BPAG2, and β-actin were amplified with TaKaRa Ex Taq Hot Start Version, and PCR products were analyzed by electrophoresis on 1% agarose gels. All procedures were performed according to the manufacturer's instructions.

The primers were as follows:

Mouse bpag1-f:5′- TTGGAACAGACCTGGAGACC-3′
Mouse bpag1-r:5′- GTTCAGCCTTTCCATTTCCA-3′
Mouse tbc1d13-f:5′- AGGCCAACATGGGTGTATTC -3′
Mouse tbc1d13-r:5′- AGGGTTTGGGTTCAGAGGAT-3′
Mouse c7orf30-f:5′- GAGGGGAAGGACGCTGAC -3′
Mouse c7orf30-r:5′- TGGAAGCATCAAATGGATCA-3′
Mouse β-actin-f:5′- CCACTGCCGCATCCTCTTCC-3′
Mouse β-actin-r:5′- CTCGTTGCCAATAGTGATGACCTG -3′
Human BPAG1-f:5′- CCAGCCCGGTTAACTATTGA -3′